

Magnetic properties of Mn impurities on GaAs (110) surfaces

M. Fhokrul Islam and C. M. Canali
*School of Computer Science, Physics and Mathematics,
 Linnæus University, 391 82 Kalmar, Sweden*
 (Dated: August 29, 2011)

We present a computational study of individual and pairs of substitutional Mn impurities on the (110) surface of GaAs samples based on density functional theory. We focus on the anisotropy properties of these magnetic centers and their dependence on on-site correlations, spin-orbit interaction and surface-induced symmetry-breaking effects. For a Mn impurity on the surface, the associated acceptor-hole wavefunction tends to be more localized around the Mn than for an impurity in bulk GaAs. The magnetic anisotropy energy for isolated Mn impurities is of the order of 1 meV, and can be related to the anisotropy of the orbital magnetic moment of the Mn acceptor hole. Typically Mn pairs have their spin magnetic moments parallel aligned, with an exchange energy that strongly depends on the pair orientation on the surface. The spin magnetic moment and exchange energies for these magnetic entities are not significantly modified by the spin-orbit interaction, but are more sensitive to on-site correlations. Correlations in general reduce the magnetic anisotropy for most of the ferromagnetic Mn pairs.

I. INTRODUCTION

Since the discovery of ferromagnetic order in Mn-doped GaAs with a Curie temperature above of 100 K,¹ research in dilute magnetic semiconductors (DMS) has developed into an important branch of material science. Early work, besides being aimed at understanding the physics of (Ga, Mn)As was strongly focused on the goal of achieving room-temperature ferromagnetism in this prototype DMS. Although this goal seems now of difficult realization, (Ga, Mn)As and DMSs in general still attract a lot of attention both for fundamental science and applications (e.g. in spintronics).^{2,3} From the point of view of theory, intense effort based on both phenomenological models^{4–13} and ab-initio calculations^{14–18} has lead to undoubted progress in understanding the origin and the properties of ferromagnetism in (Ga, Mn)As. Yet, some fundamental aspects related to the microscopic mechanism remain controversial and are still strongly debated.^{19–21}

On the experimental front, recent scanning tunneling microscopy (STM) studies in (Ga, Mn) As have been able to visualize the spatial structure of the acceptor wavefunctions at doping concentrations near the metal-insulator transition and shown that it has a multifractal character, possibly indicating carrier correlations.²² Similar STM experiments have been carried in the last few years at very low doping concentrations,^{23–29} probing specifically the properties of isolated single and pairs of substitutional Mn impurities in GaAs. Apart from helping understand the very dilute limit of magnetic semiconductors, these studies are interesting *per se*,³⁰ in that individual magnetic impurities in semiconductors represent novel nano-magnetic entities with un-

usual properties and promising applications.³⁰ The high-resolution STM measurements provide detailed information on e.g. the character of the wavefunctions of single magnetic dopants in semiconductors, and the exchange interaction between two nearby isolated magnetic impurities interacting via their associated itinerant holes.

Theoretical approaches based on tight-binding models^{31,32} have so far provided a clear picture of many of the STM experimental findings on single dopants, including the anisotropic form of the Mn acceptor wavefunction and its dependence on the Mn spin direction,^{32,33} and the dependence of the exchange coupling between two Mn impurities in GaAs on pair orientation and atomic separation.^{25,31,34,35} Tight-binding calculations are also able to provide a description of how the properties of the Mn acceptor state depend on the distance of the magnetic impurities from the surface layer³², which is in qualitative agreement with experiment.^{29,36}

First-principles calculations based on density functional theory (DFT) play an important role in the theoretical study of DMS.¹⁸ With the caveat of the well-known difficulties of DFT of predicting correctly band gaps semiconductor and dealing with localized strong correlations at the impurity sites, DFT-based first-principle calculations have become a very powerful tool to investigate the electronic structure and the magnetic properties of DMS. For the specific case of the effective exchange coupling between two isolated magnetic impurities in *bulk* GaAs, earlier DFT calculations^{14,15} have provided useful information on its microscopic origin and its strong anisotropic character with respect to pair orientation. DFT techniques have also been used to simulate STM images of the Mn acceptor states,^{16,37}

both for interstitial and substitutional impurities, yielding results that are qualitatively consistent with experiment.⁵⁰

A quantity that so far has not been thoroughly investigated by first-principle methods is the magnetic anisotropy energy, particularly for the case of magnetic impurities located close to the symmetry-breaking surface which provides STM access. The magnetic anisotropy is a very important quantity, particularly when it comes to utilizing these nanomagnets in spintronics applications. Indeed, the minima in the magnetic anisotropy landscape determine the direction of the magnetization. In DMSs the magnetic anisotropy barriers can be efficiently varied with an external electric field, which can change the carrier concentration, via the spin-orbit interaction (SOI).² Therefore it is in principle possible to control and manipulate the magnetization direction solely by means of an electric field. Tight-binding calculations provide an estimate of the magnetic anisotropy for Mn impurities on the GaAs surface.³² Nevertheless, microscopic calculations based on first-principles approach are certainly desirable.

In this paper we present first-principles calculations of the magnetic properties for single and pairs of substitutional Mn impurities on the (110) surface of GaAs, which is the most common cleaved surface employed in cross sectional STM studies. We focus, in particular on the anisotropic characteristics of important magnetic quantities, such as total energy, spin and orbital moments and exchange coupling, resulting from the interplay of SOI and symmetry-breaking surfaces. Since on-site self-interaction corrections on magnetic impurities are crucial to correctly describe the Mn d electronic states in GaAs, we carry out our calculations in the framework of the Generalized Gradient Approximation + Hubbard U (GGA + U) scheme, and we examine the effect of on-site correlations on the anisotropic properties.

We find that the typical magnetic anisotropy energy for a single substitutional Mn impurity on the (110) plane is of the order one 1 meV, with easy axis in the plane. These conclusions are only slightly affected by the presence of the Hubbard U term, which on the other hand modifies the value of the total spin moment. The calculation of the total orbital moment yields very small values, ascribable to contributions coming predominately from the acceptor p states and, to a lesser extent, from the Mn d states. For two nearby Mn impurities, the magnetic anisotropy/atom is of the same order of the single-impurity anisotropy. The effective exchange coupling between the two Mn is typically ferromagnetic (i.e., the energetically stable configuration has two

moments aligned parallel), and strongly anisotropic with respect to pair orientation in the surface and atom separation. These anisotropies are mainly a result of the GaAs crystal structure and symmetry-breaking surface. The effect of the SOI on the exchange constant and spin moment is, as expected, rather small.

On the other hand, the exchange coupling is affected by the Hubbard U term, particularly when the Mn atoms are at the shortest possible separation. This effect persists at larger separations for a Mn pair in the bulk, but it is significantly smaller for a Mn pair on the surface, for which the Mn acceptor wavefunctions tend to be more localized.

The paper is organized as follows. In Sec. II we discuss some technical aspects of the DFT calculations presented in this paper. Sec. III A contains the results of our numerical simulations for individual Mn impurities on a (110) GaAs surface. The properties on a Mn pair, with a discussion of the effective exchange interaction is presented in Sec. III B. Finally Sec. IV summarizes our work and discusses its implications for the physics of magnetic impurities in semiconductors and semiconductor spintronics.

II. COMPUTATIONAL DETAILS

The density functional theory (DFT) calculations in this work are performed using the generalized gradient approximation (GGA) with Perdew-Burke-Ernzerhof (PBE) exchange-correlation functional.³⁸ For most part of the numerical calculations the method of full potential Linearized Augmented Plane Wave with local orbitals (LAPW+lo), as implemented in WIEN2k, is used.³⁹ Because of the time-expensive nature of the plane wave method, we have used the SIESTA⁴⁰ ab-initio package for relaxing the surfaces in our calculations, SIESTA employs pseudo potentials and a numerical basis set. The relaxed coordinates are then used as an input for the WIEN2k calculations.

The (110) surface of GaAs for our calculation is constructed by cutting the bulk crystal along $< 110 >$ direction. The surface supercell consists of six layers with 18 atoms at each layer ie total of 96 atoms. A vacuum of 25 Bohr is added along the surface as shown in Fig. 1.

To study the effect of an isolated Mn impurity on the surface we have replaced one Ga atom from the center of the top layer, as shown in Fig. 1. To calculate the anisotropy energy we have calculated the effect of SOI for different magnetization directions, namely $< 100 >$, $< 001 >$, $< 011 >$ and $< 010 >$ directions. The anisotropy energy is the

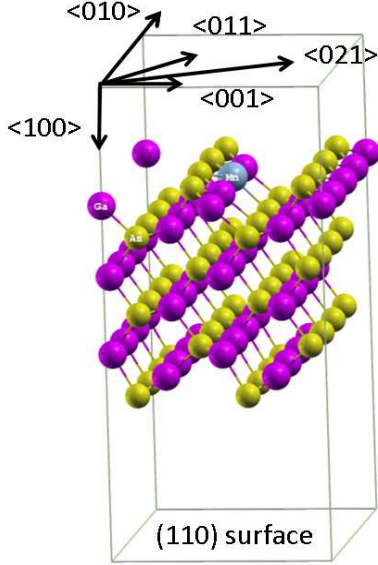


FIG. 1: A Relaxed GaAs (110) surface with a Mn impurity. The arrows indicate different crystallographic axes of the surface supercell defined for this work.

difference between the largest and the smallest energies. The spin-orbit coupling in Wien2k is incorporated via a second variational step using scalar relativistic eigenstates as basis.⁴¹

The strong correlation among the d electrons of Mn atoms is accounted for by adding an orbital dependent potential U for the d shell electrons. The value of U for Mn is usually chosen between 3 and 4 eV to match photoemission spectra and in our calculation we have used $U = 4$ eV following K. Sato *et al.*¹⁸

To study the dependence of the exchange energy on the pair orientation we replace two Ga atoms by two magnetic impurities. One of the impurity atoms is kept fixed at the top layer of the supercell (front left corner of Fig. 1) and the position of the second one is varied along different crystallographic directions, namely $[001]$, $[010]$, $[011]$ and $[021]$. In this paper we only consider the case in which the spin magnetic moments of the two impurities are collinear. The exchange energy for each pair orientation is calculated as the difference in energies of the supercell when the spins of the impurity atoms are arranged parallel and antiparallel. For the anisotropy calculation with two impurities we have followed the same procedure as we have done for the single impurity case.

Since the size of the surface supercell is large, we have used only one k-point for these calculations and self-consistency is achieved when total energies are

converged to within 0.01 mRy or better and charge is converged to 0.001e or better.

III. RESULTS

A. Single Mn on (110) GaAs surface

1. Electronic structure

We start by analyzing the main features of the electronic structure when an individual Mn impurity replaces a Ga atom on the (110) surface of GaAs. A Mn atom introduces a magnetic moment in the host material. This can be seen by plotting the partial Density of States (DOS) for the Mn d-levels as shown in Fig. 2. Intra-atomic exchange interactions, responsible for Hund's first rule, split the majority (up-spin) from the minority (down-spin) d-states, so that the former end up – almost entirely – below the Fermi level and the latter above, thus giving rise to a localized spin moment in the system. In Fig. 2 we also show the effect of on-site correlations on the d-orbital partial DOS, included via a Hubbard U term in the GGA calculations. Clearly correlations split majority and minority states further apart, pushing the former deeper below the Fermi level. As discussed below, correlations also decrease the small peak in the partial DOS at the Fermi energy as shown in the inset of Fig. 2.

The second effect caused by a substitutional Mn impurity in GaAs is the introduction of a p-like acceptor (hole) state in its surroundings. This can be seen by plotting the p-orbital partial DOS at the Mn nearest-neighbor As sites, as shown in Fig. 3. As a comparison, in Fig. 3(a) the p-orbital partial DOS at an As site is plotted for pure GaAs (i.e., when the Mn is replaced by a Ga atom). There we can see the expected (full) valence and (empty) conduction band, with a Fermi level in the middle of the energy gap that separates them. When the Mn is present, the top of the valence band spin polarizes as a result of the hybridization between the As p orbitals with the Mn d-orbitals. In Fig. 3(b) we can see that the spin-up component (i.e., parallel to the Mn spin moment) of the As p-orbital partial DOS has a broad peak centered at the Fermi energy. The corresponding spin-down component is instead pushed below the Fermi energy, causing an effective exchange splitting between up and down states of the order of ~ 0.6 eV.

The spin-polarized states just above E_F can be identified with the acceptor hole states associated with the Mn impurity. These states are clearly the result of a moderate hybridization between spin po-

larized localized Mn d orbitals with p orbitals primarily located on the neighbor As atoms. Note that the DOS of p character is larger than the d contribution. This feature will have an impact on the nature of the anisotropy energy discussed below. The inset of Fig. 2 shows that on-site correlations decrease the majority d partial DOS at the Fermi energy. As a result, the hybridization of the hole state with the d orbitals decreases, and the acceptor becomes less localized on the Mn.

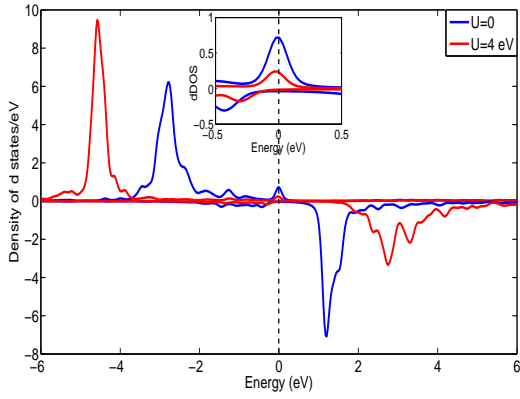


FIG. 2: (Color online) The density of Mn d states calculated with $U=0$ (blue-dark line) and $U=4$ eV (red-gray line) respectively. The inset shows the DOS near the Fermi level.

It is useful to look more carefully at the effect of the Hubbard correlations on the properties of the hole state. In Fig. 4 we plot the discrete eigenvalue energies⁵¹ for the states in the surroundings the GaAs energy gap, for pure GaAs (red curve) and for the case in which a Mn impurity is present (blue and green curves). As a result of the Mn presence, acceptor states appear in the gap of the host material. Specifically, we find two energy levels located a few hundred meV above the GaAs valence-band edge. We identify the topmost of these two levels as the acceptor state, occupied by a hole. The energy immediately below corresponds to the highest occupied (by an electron) level. Note that, with the exception of one level deep in the valence-band, the emergence of these two mid-gap levels is the only important qualitative difference that distinguishes the spectrum of the system in the presence of the Mn impurity from the one of pure GaAs. As shown in the figure, on site U correlations have an effect on these two impurity levels, slightly decreasing their energy toward the valence band-edge. The sensitivity of the acceptor energies to the Hubbard U parameter, indicates that these levels are indeed moderately hybridized with the Mn d orbitals.

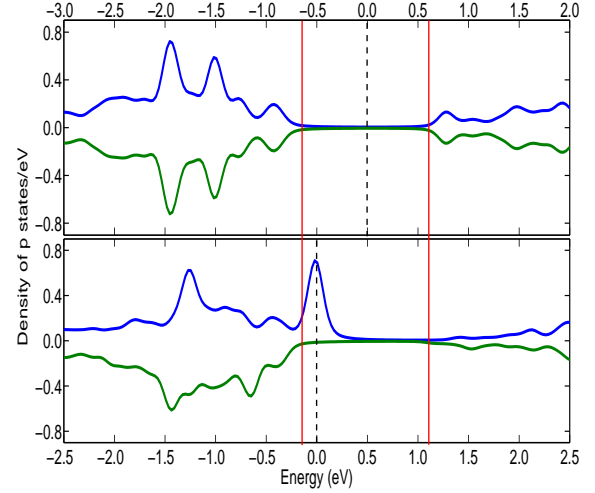


FIG. 3: (Color online)(Top) The density of As p states of pure GaAs surface. (Bottom) The p partial DOS of the same As atom when a nearby Ga atom is substituted by a Mn atom. The vertical dashed line in both panels represents the Fermi energy. The two vertical red lines delimit the energy-gap region for pure GaAs, which is clearly identifiable in the top panel. To compare the two cases, we have aligned the edge of the two conduction bands.

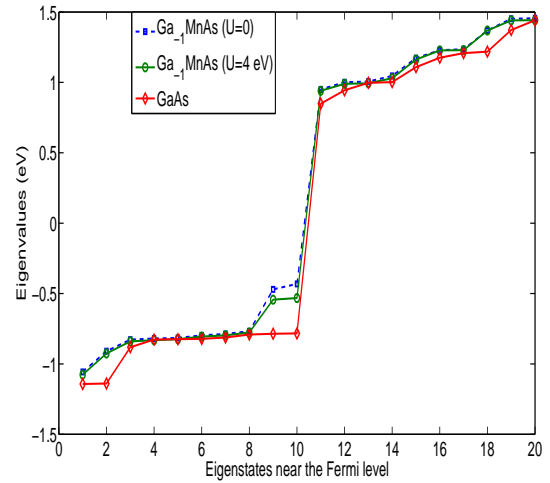


FIG. 4: (Color online) Eigenvalue energies of eigenstates in the surroundings of the GaAs energy gap. The red (gray line) is for pure GaAs. The blue (solid black) and green (dashed) curves are for the case when a surface Mn impurity is present (solid black curve) or not (dashed green). Note the appearance of the hole acceptor state in the gap, a few hundred meV above the GaAs valence-band edge. The acceptor state energy is moderately affected by the presence of Hubbard U correlations, a sign that this state is in part hybridized with d -states.

Energy (eV)	Atom	$ \psi_{\text{atom},\mu} ^2$		
		Total	p	d
-0.7681 (valence)	Mn	0.002	0.000	0.002
	As1	0.004	0.004	0.000
	As2	0.004	0.004	0.000
-0.4700 (highest occ.)	Mn	0.102	0.029	0.073
	As1	0.101	0.100	0.001
	As2	0.099	0.098	0.001
-0.4321 (hole)	Mn	0.116	0.017	0.095
	As1	0.069	0.065	0.000
	As2	0.070	0.066	0.001
0.9500 (conduction)	Mn	0.001	0.000	0.001
	As1	0.004	0.004	0.000
	As2	0.004	0.004	0.000

TABLE I: Square of the wave function, $|\psi_{\text{atom},\mu}|^2$, of different energy levels near E_F , including the acceptor hole state, calculated at the Mn site and its two As nn on the (110) surface. The $\mu = p, d$ orbital character contributions are separately specified on the second and third column. Here the Hubbard $U = 0$. The first level belongs to the host valence band, while the last level is in the conduction band. The bold faced numbers correspond to the acceptor hole state. The level immediately below the hole state corresponds to the highest occupied level. Both states are inside the energy gap. See Fig. 4.

In order to understand further the effect of correlations on the hole state, in Tables I and II we display the square of the wave function for a few levels around the Fermi level at the Mn site and at the site of its two As nearest neighbors (nn) on the (110) surface. The partial contribution of a given orbital character (p or d) is shown together with their sum for a given atom. Table I and II correspond to the cases of $U = 0$ and $U = 4$ respectively. As anticipated above, we can see that the hole state comes about from the hybridization of the Mn d orbitals with the p states of its two As nn. We note that with $U = 0$ (see Table I) the hole state is predominantly of d character but hybridized with As p states. With U turned on (see Table II), the d character of the hole state at the Mn site decreases, while the p character weight on the nearby As is essentially unchanged. This is a clear indication that the hole state is pushed out into the interstitial region between Mn and its nearby As atoms by on-site correlations, namely it acquires a less localized and more itinerant character.

As shown by Mahadevan *et al.*,¹⁵ on-site correlations are known to increase the itinerant character of the hole state for Mn impurities in bulk GaAs¹⁵. To understand the difference in the nature of the

Energy (eV)	Atom	$ \psi_{\text{atom},\mu} ^2$		
		Total	p	d
-0.7764 (valence)	Mn	0.001	0.000	0.001
	As1	0.005	0.005	0.000
	As2	0.005	0.005	0.000
-0.5431 (highest occ.)	Mn	0.052	0.029	0.023
	As1	0.107	0.107	0.000
	As2	0.103	0.103	0.000
-0.5316 (hole)	Mn	0.052	0.016	0.032
	As1	0.069	0.065	0.000
	As2	0.073	0.069	0.000
0.9400 (conduction)	Mn	0.001	0.000	0.000
	As1	0.004	0.002	0.000
	As2	0.004	0.004	0.000

TABLE II: Square of the wave function, $|\psi_{\text{atom},\mu}|^2$, as in Table I, but with $U = 4\text{eV}$.

hole state in bulk and surface, we have calculated the Mn acceptor hole properties of bulk GaAs. We use a 64 atom supercell with a single Mn impurity in the middle. The occupancies of the hole state at the Mn site, its two nn and two next nearest neighbor (nnn) As sites are tabulated in Table III. It is evident that when U is turned on the hole state extends over nnn As sites. A similar result is obtained by Mahadevan *et al.*¹⁵ in their bulk GaAs calculations. In the surface calculations, although the occupancies of the hole state at the nnn As atoms on the surface layer slightly increases, the effect is less pronounced in the surface compared to the bulk. We conclude that for a Mn impurity on the surface, the associated acceptor state remains predominantly localized in the interstitial region between the Mn and the two nn As atoms. Consequently, the hole state for a Mn on the (110) is energetically a rather deep impurity, compared to the case of Mn in bulk GaAs. The localized character of the hole wavefunction for a surface Mn and its relatively large binding energy are supported by both STM experiments^{25,29,36} and tight-binding calculations.³²

Finally, Tables I and II show that on-site correlations also decrease the Mn d -orbital contribution of the highest occupied level by approximately 50% (compare Table I and, II). As evident from the inset of Fig. 2, this effect involves primarily majority spin states at the Fermi level.

The electronic properties the Mn acceptor hole state are only weakly affected by the direction of the Mn moment direction as a result the SOI. In Fig. 5 we plot the difference in the p partial DOS for one of the two As nearest-neighbor, for two directions of the

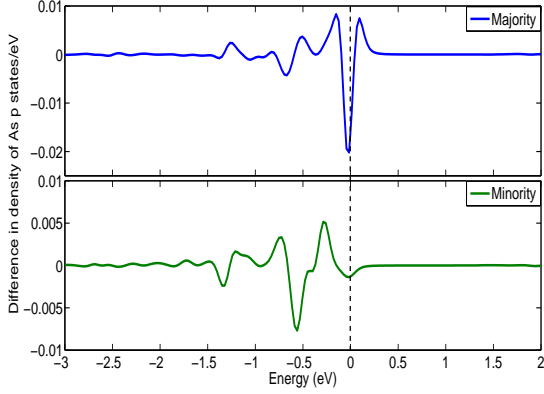


FIG. 5: (Color online) Difference in the As p density states, for two directions of the magnetization, $\langle 001 \rangle$ and $\langle 010 \rangle$, in the presence of SOI and for $U = 4$ eV.

Atom	$ \psi_{\text{atom},\mu} ^2$					
	$U=0$			$U=4$ eV		
	Total	p	d	Total	p	d
Mn	0.176	0.024	0.151	0.050	0.013	0.036
As1+As2 (nn)	0.098	0.092	0.002	0.078	0.076	0.002
As3+As4 (nnn)	0.006	0.006	0.000	0.018	0.018	0.000

TABLE III: Properties of the hole state, as in Tables I, II, but for a Mn in *bulk* GaAs on the (110) plane. As3 and As4 are the two next nn As atoms of the Mn on the (110) plane.

magnetization, $\langle 001 \rangle$ and $\langle 010 \rangle$ respectively. The SOI induced change is only a few percents. We will see below that the magnetic anisotropy energy can be explained by this direction dependence. This is consistent with tight binding calculations³² for a substitutional Mn on the (110) surface, which show that the square of acceptor hole wave function is anisotropic in space, but does not change significantly with the Mn moment direction.

2. Spin magnetic moment

The spin magnetic moment M_S for one Mn on the (110) GaAs surface is given in Table IV. When $U = 0$ the spin moment on the Mn is $M_S = 4.05$ in units of the Bohr magneton μ_B . A close inspection shows that there are 4.39 majority-spin and 0.42 minority-spin d electrons on the Mn atoms. The remaining small contribution 0.08 to the Mn spin moment comes from s electrons. The deviation from

Spin moment, μ_B	M_S	M_S^{Tot}
$U = 0$	4.05	4.07
$U = 4$	4.46	4.21

TABLE IV: Spin magnetic moment on Mn (M_S) and total spin moment per unit cell (M_S^{Tot}) in Bohr magnetons.

the Mn atomic limit of $5 \mu_B$ is due to the acceptor hole being in part localized on the Mn. When $U = 4$, the spin on the Mn increases from 4.05 to 4.46 due to the concomitant increase of the majority-spin and decrease of the minority-spin d electrons. The increase of the spin moment on the $3d$ adatom as a result of correlations is expected, since the Hubbard U term tends to localize the d electrons. Notice however that, in this case, the total magnetic moment per unit cell $M_S^{\text{Tot}} = 4.21$ is smaller than M_S . Indeed M_S^{Tot} includes also a negative contribution from the p orbitals on the nearby As atoms, which are partly spin polarized in the opposite direction of the Mn d spin moment, as shown in Fig. 3. The results in Table IV are very weakly affected by SOI. In particular, the value of the spin magnetic moment does not show any appreciable anisotropy with respect to its direction.

3. Orbital moment

Next we discuss the orbital magnetic moment. An isolated Mn atom has the spin-majority d levels fully occupied and the spin-minority states empty. As a result the total orbital moment M_L is zero. Note that each of the individual degenerate d orbitals carries a unit of orbital angular momentum equal to $m_l = 0, \pm 1, \pm 2$. When a Mn atom is substituted for a Ga atom in GaAs, the crystal field of the host material removes the degeneracy of the Mn d levels and each orbital moment of the perturbed states becomes quenched. The effect of SOI is to reduce quenching and to restore, at least partially, the individual orbital moments by mixing different d states. However, since the spin-majority d manifold is still practically fully occupied while the minority-spin is empty, we expect that, even in the presence of SOI, the total orbital moment M_L on the Mn atom to be very small. On the other hand, an acceptor Mn impurity introduces also an itinerant hole state, which is a state with a predominant p character and as such should have an orbital magnetic moment. Thus we expect that the valence band states, filled up to the Fermi level, should generate a net orbital moment equal and opposite to the orbital moment of the hole. These simple considerations are fully supported by

Magnetization direction	Orbital moment, μ_B			
	$U=0$		$U=4$ eV	
	M_L^d	$M_L^{p,\text{Tot}}$	M_L^d	$M_L^{p,\text{Tot}}$
$\langle 001 \rangle$	0.015	-0.028	0.007	-0.031
$\langle 010 \rangle$	0.007	-0.016	0.000	-0.019

TABLE V: Orbital d magnetic moment on Mn (M_L^d) and total p orbital moment per unit cell (M_L^{Tot}) in Bohr magnetons calculated for two directions of the magnetization, $\langle 001 \rangle$ (easy) and $\langle 010 \rangle$ (hard). The minus sign indicates that the orbital moment points in the opposite direction of the spin orbital moment.

the DFT calculations. Results are summarized in Table V.

We find that the calculated orbital moment of the Mn d states is indeed very small and slightly anisotropic: for the magnetization directed along $\langle 001 \rangle$ (which turns out to be the easy direction, see next Section) $M_L^d \approx 0.015\mu_B$; for the magnetization directed along $\langle 010 \rangle$ (one of the hard axis), M_L^d is about $0.007\mu_B$. The total p orbital moments of the unit cell for easy and hard directions are -0.028 and $-0.016\mu_B$, respectively. These value are larger than the d orbital moment but still considerably small. The negative moment implies that orbital moment is opposite to the spin moment of the system. The orbital moment of the hole state, on the other hand, is aligned parallel to the spin moment and, as expected from the discussion above, almost exactly cancels the orbital moment of the whole cell. The largest contribution to the moment comes from the two As (14% each) nearest to Mn (5%) and one As in the first subsurface layer (12%). For the easy axis, apart from these atoms other subsurface layer As atoms along $[111]$ direction also have finite contribution to the orbital moment, suggesting that the hole state is extended along that direction. For the hard axis the direction of extension of the hole state remains the same but the largest contribution to the p orbital moment comes from the first subsurface layer As atom (16.5%), while two surface As atoms contribute only 7.4% each with negligible contribution from Mn. The on-site correlation, U , has very little effect on p orbital moment of the whole cell but the d orbital moment of Mn becomes vanishingly small with $U = 4$ eV.

On the basis of these results for the spin and orbital magnetic moment, we can conclude that for a Mn impurity on the (110) surface, the total magnetic (spin plus orbital) moment of the system is approximately $4\mu_B$. Assuming that the total magnetic moment is a combined effect of the Mn and the acceptor hole, we can imagine to assign an effective

”spin” $J = 2$ to this magnetic entity composed of the Mn impurity and its hole. The effective spin J can be understood as a result of the Mn spin ($S = 5/2$) antiferromagnetically coupled to the spin of the hole state ($s = 1/2$). For both Mn and acceptor the associated orbital moment is small, although not entirely negligible for the hole. These results can be compared with the well-known situation of a substitutional Mn impurity in bulk GaAs. In that case electron-spin resonance⁴² and infrared spectroscopy absorption experiments,⁴³ together with theoretical considerations, have shown that the the total spin of the (Mn + hole) complex is $J = 1$, and it results from the antiferromagnetic coupling of the Mn spin moment $S = 5/2$ and the hole total angular momentum $j = s + l = 1/2 + 1 = 3/2$. Our calculations indicate that when a Mn replaces a Ga on the Mn surface, the orbital moment of the associated acceptor hole is small, most likely due to the fact that the high (tetragonal) symmetry experienced by the hole in the bulk GaAs is strongly reduced by the surface. This reasoning and conclusions are in agreement with a recent theory⁴⁴ that identifies the total effective ”spin” of the (Mn + hole) acceptor magnet with a Berry phase Chern number J . Tight-binding calculations implementing this theoretical approach find that J is 2 for a Mn near the (110) surface, due to the quenching of the orbital moment of the acceptor hole state.

4. Magneto-crystalline anisotropy

We now discuss the magnetic anisotropy energy (MAE), defined as the dependence of the ground-state energy on the magnetization direction. The most important contribution to the MAE is the magneto-crystalline anisotropy caused by the SOI. For a single substitutional Mn impurity in bulk GaAs the tetragonal symmetry of the host lattice implies that the MAE is essentially zero. On the surface however, the symmetry is broken, and the anisotropy is finite. Note that surface relaxation and strain (e.g. induced by interfaces with other lattices or by external electric fields) can enhance the anisotropy considerably.

Although it is common to calculate the MAE using an approximate method known as magnetic force theorem,⁴⁵ we have first estimated it by calculating the total energy including SOI as a function of different magnetization directions shown in Fig. 1. The anisotropy barrier between two magnetization directions, \hat{M}_S and \hat{M}'_S , is defined as the difference in

MAE	$U = 0$	$U = 4$ eV
$E(\langle 010 \rangle) - E(\langle 001 \rangle)$	1.17	1.13
$E(\langle 100 \rangle) - E(\langle 001 \rangle)$	0.17	0.16
$E(\langle 010 \rangle) - E(\langle 100 \rangle)$	1.00	0.97

TABLE VI: Magnetic anisotropy energy (in meV) for one substitutional Mn impurity on the (110).

total energy between these two directions,

$$\Delta E_A = E(\hat{M}_S) - E(\hat{M}'_S) \quad (1)$$

In our calculations we find that the total energy $E(\hat{M}_S)$ is minimal when \hat{M}_S is along the $\langle 001 \rangle$ direction (easy axis) and maximal when \hat{M}_S is along the $\langle 010 \rangle$ direction (hard axis), both of which lie in the (110) plane. The largest MAE barrier that we find from our calculation is 1.17 meV when $U = 0$ and it decreases slightly to 1.13 meV when $U = 4$ meV. A summary of the magnetic anisotropy energy for different magnetization orientations is presented in Table VI. Notice that the MAE barrier to rotate the magnetic moment from the easy axis and align it along the $\langle 100 \rangle$ direction (perpendicular to the surface) is only 0.16 meV.

It is now instructive to look at the MAE from the point of view of the magnetic force theorem.⁴⁵ This amounts to express the total energy $E(\hat{M}_S)$ as the sum of the magnetization-dependent Kohn-Sham band eigenvalues, ϵ_n

$$E(\hat{M}_S) = \sum_n^{\text{occ}} \epsilon_n(\hat{M}_S) \quad (2)$$

where the sum is over the occupied KS eigenvalues. By introducing the (magnetization dependent) DOS, we can rewrite $E(\hat{M}_S)$ as

$$E(\hat{M}_S) = \int_{\epsilon_B}^{\epsilon_F} (\epsilon - \epsilon_F) \rho(\hat{M}_S) d\epsilon, \quad (3)$$

where ϵ_B is the bottom of the valence band and ϵ_F is the Fermi energy. We can then write the MAE barrier as

$$\text{MAE} = \int_{\epsilon_B}^{\epsilon_F} (\epsilon - \epsilon_F) [\rho(\hat{M}_S^{\text{hard}}) - \rho(\hat{M}_S^{\text{easy}})] d\epsilon. \quad (4)$$

It turns out that the integrand of Eq. 4 – the change in band energy upon varying the direction of the magnetization – can be of either sign. When these changes are summed up for all occupied states

we can expect large cancellations, so that what matters in the end is the dependence of the band energies around the Fermi energy.

We can now surmise that the magnetic properties of the system including the variations of the DOS on the magnetization direction, should mainly affect the region of the Mn and its immediate surroundings. As we can see in Fig. 2 and Fig. 3, the projected DOS at the Fermi energy for the Mn impurity and its nearest-neighbor As atoms shows that the dominant contribution come from the states of p character primarily located on the nn As. An inspection of the p DOS for many other atoms in the supercell shows that, besides the Mn and its two nn As atoms, only the As atoms in the first sub-layers closest to the Mn have a finite contribution at E_F , which becomes progressively smaller the further the As is from the Mn. Thus we can expect that the MAE is primarily controlled by the p orbital components of the band energies at E_F located at these atoms.

Indeed, if we calculate the MAE by integrating Eq. 4 for all band energies within a few eVs of the Fermi level for the Mn and the nearby As atoms, including those As on the sub-surface layers, we obtain $\text{MAE} \approx 2.8$ meV, which differs only by a factor of 2 from the more precise estimate obtained above. The two As atoms nearest to Mn on the surface layer contribute about 64% of the MAE, whereas the As on the first sub-surface layer and closest to Mn contribute about 17%, with Mn d level contributing about 18%.

Furthermore, tight-binding calculations show that the MAE obtained by summing up magnetization-dependent energy variations for all occupied levels is equal and opposite of the anisotropy energy for the acceptor hole state only³². If we compute the integral $\text{MAE}_{\text{hole}} = \int_{\epsilon_F}^{\epsilon_{\text{hole}}} (\epsilon - \epsilon_F) [\rho(\hat{M}_S^{\text{hard}}) - \rho(\hat{M}_S^{\text{easy}})] d\epsilon$, where ϵ_{hole} extends up to the limit of the hole-peak DOS (see Fig. 3), we find $\text{MAE}_{\text{hole}} \approx -2.25$ meV, which has the expected opposite sign and is very close in magnitude to the MAE calculated summing all the energy shifts up to E_F . About 68% of the hole anisotropy comes from the two As atoms nearest to Mn on the surface layer, while the Mn and the first sub-surface layer As contributions are 14% and 16% respectively.

Note that in the previous section we found that a similar property holds for the orbital moment of the system: the total orbital moment, primarily located on the Mn, the nn As, and the closest As in the immediate subsurface layers, is equal and opposite of the contribution of the hole-state orbital moment, located primarily on the same atoms.

The difference in MAE calculated from the total

energy difference (Eq. 1) and magnetic-force theorem (Eq. 4) is expected, since the latter is an approximate method, and is due to the fact that DFT calculates the groundstate energy of a many-body system in a physically meaningful way, whereas individual single-particle energies are rather a mathematical artifact used to solve the Kohn-Sham equations.

In applying the magnetic-force theorem, we have disregarded the contribution of all the other atoms in the supercell, under the assumption that their contributions are small around the Fermi level. In fact, we have explicitly verified that the p partial DOS of these As atoms have a negligible value around the Fermi level and the integration of Eq. 4 around the Fermi level gives insignificant contribution to the MAE. This is, however, not the case if we include the band energies deep in the valence band in the calculation of the MAE, which appear to give some contribution for all atoms. We don't believe that this is an indication of a finite contribution to the MAE coming from atoms far way from the Mn, but rather a sign of the non-sufficient accuracy in the computation of the SOI-induced shift in the states deep in the valence band.

At this point it is interesting to investigate more closely the connection between the anisotropy properties of the total energy and the orbital moment. The discussion above already suggests that these two quantities should be related. According to the perturbative (in SOI) analysis by P. Bruno,⁴⁶ there is an approximate relationship between the MAE and the orbital moment anisotropy

$$E(\hat{M}_S) - E(\hat{M}'_S) = -\frac{\xi}{4} [M_L(\hat{M}_S) - M_L(\hat{M}'_S)] \quad (5)$$

where ξ is the SOI coupling strength. In particular, Eq. 5 implies that ΔE_A is proportional to the difference in the orbital moment for the spin moment in the easy and hard direction. The orbital moment calculation clearly shows that the orbital moment anisotropy of the hole comes mainly from As p states with a small contribution from the Mn d states. Using the SOI coupling constant of As, $\lambda_{As}=140$ meV,⁴⁷ Bruno formula yields $\Delta E_A^{\text{Bruno}}=0.35$ meV. This is approximately a factor of 3 smaller than MAE calculated using DFT. The Bruno formula has been investigated recently for systems consisting of magnetic impurities on metal⁴⁸ and insulator surfaces.⁴⁹ In some cases the relationship seems to work satisfactorily, in other it fails. As far as we know a similar analysis for magnetic acceptor impurities in semiconductors has not been carried out. This situation is different from an ordinary magnetic impurity on an insulator for example, in

that, an important role in the magnetic properties of the system is now played by the itinerant acceptor hole. Our analysis shows that orbital moment of the hole state is certainly related to the magnetic anisotropy energy, as in Eq. 5, albeit with a renormalized SOI coupling strength. This might be an indication that our DFT calculations underestimate the orbital magnetic moment due to the lack of orbital dependence of the exchange potential.⁴⁸

The electronic and magnetic properties of a single Mn impurity on the (110) GaAs surface calculated here are in general, in good agreement with tight-binding based calculations by Strandberg *et al.*³² In particular, the value of the magnetic anisotropy energy barrier are pretty close for the two approaches ≈ 1 meV. However, details of the magnetic anisotropy energy landscape are different. While in our calculation we have both easy and hard axes in the (110) plane, Strandberg *et al.* find an easy axis that makes an angle 45° with the surface. The difference may stem from the fact that they have used much larger clusters and hence their system is much more diluted than the system used in this calculation.

B. Mn pair on (110) GaAs surface

In this section we discuss the properties of a pair of substitutional Mn impurities on the (110) surface. It turns out that the electronic and magnetic properties are quite similar to the ones of individual Mn impurities. After a brief summary of these properties we will concentrate on discussing the effective exchange coupling and the magnetic anisotropy of the Mn pair and their dependence on atom separation and orientation on the (110) surface.

1. Electronic structure and spin moment

The d partial DOS for different pairs of Mn impurities shows a similar pattern as in the case of a single impurity, both with $U = 0$ and $U = 4$ eV. In particular there is rather weak dependence on atom separation and pair orientation with respect to the surface crystal structure. As for the case of individual Mn impurities, the effect of U is to reduce the intensity near the Fermi level and to further split the main majority and minority peaks, pushing the former below the Fermi level and the latter above. Fig. 6 shows the local density of d states of one of the two Mn atoms (up spin only) for different pairs on the surface, when $U=4$ eV. While the main majority peak is insensitive to the orientation of the Mn pairs,

the partial DOS is rather wide at the Fermi level for the [010] orientation because of the smaller distance between the two Mn atoms for this orientation.

The properties of the spin magnetic moment (per atom) are essentially the same as for individual Mn impurities, for all pairs on the surface. For example, the Mn spin moment is approximately equal $4 \mu_B$ when $U = 0$ and increases to $4.5 \mu_B$ when on-site correlations are included by setting $U = 4$ eV, as in the case of a single impurity.

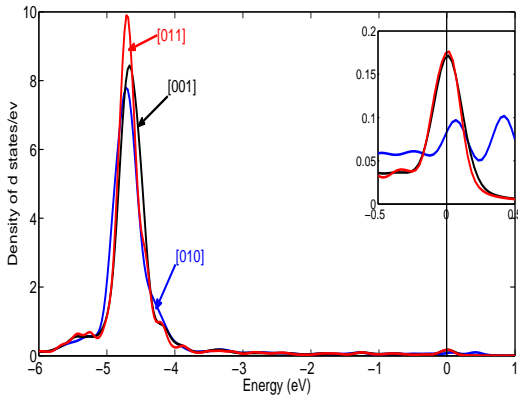


FIG. 6: (Color online) Density of d states for different orientations of a pair of Mn on (110) surface of GaAs. See Fig. 1 for different orientations of the pair relative to the crystallographic axes. The inset shows the DOS near the Fermi level.

2. Exchange interaction

A strong exchange interaction between magnetic impurities in a semiconductor is essential for its successful application as a spintronic device, since magnetic properties of semiconductors must be preserved at room temperature and above. In this work we have calculated the exchange energy between two Mn impurities on (110) surface of GaAs and have investigated the effect of correlations and SOI on exchange. The exchange energy for each pair orientation is defined as the difference in energies of the supercell when the spins of the two impurity atoms are arranged parallel and antiparallel

$$J \equiv E_{\text{cell}}^{\uparrow\downarrow} - E_{\text{cell}}^{\uparrow\uparrow} \quad (6)$$

A positive (negative) J implies that the Mn-Mn interactions are ferromagnetic (antiferromagnetic) Fig. 7 shows the dependence of the exchange constant J on the separation between the two Mn atoms

of the pair and on the pair orientation relative to the crystallographic axes of the surface.

The exchange constant J is largest for the pair with the shortest separation along the [010] direction, where the two Mn are nearest neighbors, and it decays quickly with impurity separation. The general trend and order of magnitude of J shown in Fig. 7 is in agreement with the results of tight-binding calculations, despite these are carried out for a much more dilute system, which is supposed to model the situation studied in STM experiments. Although the smaller size of the surface supercell restricts our ability to study, in detail, the orientation dependence of exchange, it is evident from the figure that the exchange constant is larger when the pair is oriented along [011] direction than when it is oriented along [021] direction, even though the distance between the Mn atoms is smaller in latter case. This is a clear indication of the strongly anisotropic nature of the exchange coupling for pairs of substitutional Mn impurities on the (110) GaAs surface. Evidence of this anisotropy was found in recent STM experiments²⁵ and is also supported by tight-binding calculations.^{25,31,34,35} We also note that as the distance between Mn atoms increases along the [010] direction, J becomes negative, i.e. the antiferromagnetic coupling of the Mn pair becomes energetically favorable. This result implies that a random distribution of impurities along different directions might reduce the overall magnetization of a dilute system.

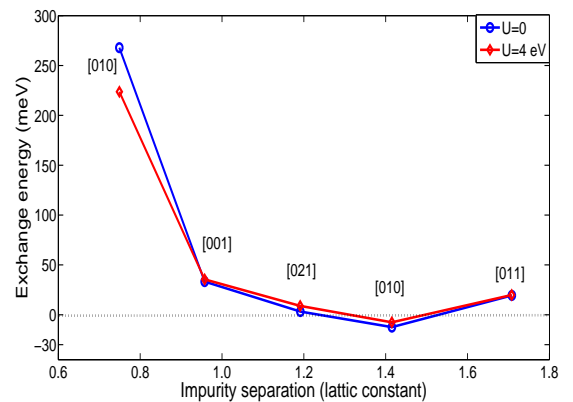


FIG. 7: (Color online) Dependence of the exchange energy constant J on the orientation and Mn-separation for a pair of Mn impurities on the (110) surface of GaAs.

As evident from Fig. 7, the effect of strong correlations, U , on the exchange anisotropy is rather small except for the shortest Mn separation where correlations *decrease* J by approximately 15%. As we have seen in the study of one Mn impurity, on-

Orientation of Mn atoms	Exchange energy, J (meV)		Magnetic moment	
	U=0	U=4eV	U=0	U=4eV
[010] ₁	267.9	223.7	4.0	4.4
[001]	33.3	35.5		
[021]	3.2	8.9		
[010] ₂	-12.4	-7.6		
[011]	19.4	19.8		

TABLE VII: Exchange energy and magnetic moment for a Mn pair on the (110) GaAs surface. The subscripts "1" and "2" in the [010] direction indicate respectively the nearest and 2nd nearest Mn atoms along that direction.

site correlations have a small tendency in delocalizing the acceptor hole around the Mn. According to theory, the acceptor hole is expected to mediate the exchange interaction among the magnetic moments of Mn pairs. Except for the shortest impurity separation, the enhanced itinerant character induced by correlations is still of limited range in space to have a noticeable effect on the exchange constant. Nevertheless, a close inspection of the numerical values of J (see Table III B 2) shows that, with the exception of the pair with the shortest separation, the effect of U is always to increase J .⁵² This is consistent with the fact that exchange mediating-hole becomes more delocalized as a result of on-site correlations.

Although the results shown in Fig. 7 are obtained in the absence of SOI, we have checked that SOI has little influence on J . For instance for the [010]₂ orientation J increases by 1-2 meV depending on the direction of magnetization, for both $U = 0$ and $U = 4$ eV.

3. Magnetic anisotropy

The MAE barrier for a pair of Mn atom on GaAs (110) surface varies from 0.44 meV to 2.67 meV depending on the orientation of the pair relative to the crystallographic axes, as shown in Fig. 8. For all pairs except for the pairs along the [010] orientation, the easy axis is found to be along $\langle 001 \rangle$ and the hard axis is along $\langle 010 \rangle$ direction. For the pair oriented along [010], while for the nn the situation is inverted (i.e., the easy axis is along $\langle 010 \rangle$ and the hard direction is along $\langle 001 \rangle$), for the next neighbor pair the easy axis is still along $\langle 001 \rangle$ but the hard axis changes to the $\langle 100 \rangle$ direction.

Our calculations also show an interesting correlation between the MAE and the exchange constant J . Comparing Figs. 7 and 8 we note that the Mn pair with the shortest Mn separation, which has the

largest J , is also the one with the smallest MAE. For all other Mn pairs for which J fluctuates around a considerably smaller value, the corresponding MAE fluctuates around 2 meV. It is remarkable that exactly the same behavior is found in tight-binding calculations,³⁵ where the value of the anisotropy for a Mn pair is also in quantitative agreement with the results presented here.

In the presence of correlations $U = 4$ eV, the MAE, in general, decreases except for the case when for the pair with the shortest Mn separation. This behavior is again consistent with the fact that, with the exception of the shortest pair separation, on-site correlations slightly increase the exchange constant J .

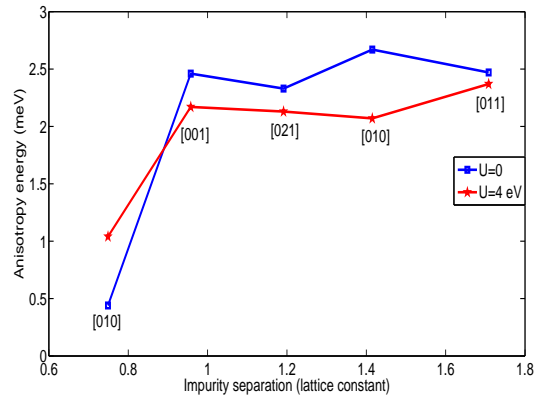


FIG. 8: (Color online) Surface anisotropy for a pair of Mn impurity on (110) surface of GaAs.

IV. CONCLUSIONS

In this work we have investigated the electronic and magnetic properties of substitutional Mn impurities on the (110) surface of GaAs, using density functional theory implementing a full potential LAPW+lo method.

A key point of our analysis has been the investigation of the Mn acceptor hole state, which appears in the GaAs energy gap. The properties of the hole state allow us to understand the salient features of a single Mn impurity in GaAs. As for a bulk Mn impurity, when the Mn is on the surface, the associated hole state is strongly anisotropic in space, but much more localized around the Mn and its two As nn than in bulk.

On site electron correlations on the Mn, included within a GGA + U framework, reduce the hybridization of the hole state with the Mn d orbitals, and

render the character of the wave function relatively more p -like and therefore slightly more delocalized. The spin magnetic moment of the Mn atom is approximately $4\mu_B$, when $U = 0$, consistent with a hole partly localized on the impurity. The Mn d moment increases to $4.5\mu_B$ when $U = 4$ eV, as a result of the more delocalized nature of the hole state. However the spin moment of the whole unit cell remains closer to $4\mu_B$.

SOI induces a small dependence of the p partial DOS at E_F on the direction of the magnetization, primarily for the As atoms closest to the Mn. With some caveats (see discussion at the end of Sec. III A 4), this dependence accounts for a calculated magnetic anisotropy energy (MAE) of approximately 1 meV and can be closely related to the anisotropy of the hole state.

The presence of SOI yields a small orbital magnetic moment in the opposite direction of the spin moment, which can again be associated to the orbital moment of the hole state. The dependence of the As p partial DOS on magnetization directions induces a very weak anisotropy in the orbital moment. We have seen that the Bruno formula relating the MAE to the orbital anisotropy is qualitatively satisfied, but underestimates the MAE.

When two Mn impurities are substituted for two Ga atoms on the (110) surface we find that the most energetically stable configuration is typically the one where the two Mn magnetic moments are oriented parallel to each other. The exchange energy J between two Mn impurities on the surface strongly depends on the orientation of the pair relative to crystallographic axes. On the other hand, the SOI-induced dependence J on the direction of the magnetization is very small. The effect of on-site correlations on J is largest for the pair along the [010] direction with nn Mn, where the exchange is reduced by 15%. For all the other pairs, correlations always enhance exchange, although the effect is typically a few percents. Finally, the MAE of a ferromagnetic Mn pair on the GaAs surface is slightly larger than that of a single impurity, except for the shortest pair for which the MAE is 0.2 meV/Mn. With U added, the MAE decreases in general.

The results presented here are in good agreement with recent tight-binding calculations carried out for individual and pairs of Mn substitutional impurities

on the (110) surface of GaAs.^{32,35,44} In particular, the MAE of a single impurity is in both cases on the order of 1 meV. Similarly the exchange energy for a Mn pair displays the same rapid decay with Mn separation and anisotropic behavior with pair orientation.

The orbital magnetic moment of the acceptor hole is very small, as a result of the surface that breaks the tetragonal symmetry of bulk GaAs, again consistent with tight-binding calculations.⁴⁴ This suggests that for a Mn impurity on the surface the “total spin” of the magnetic center composed of the Mn core and the associated spin-polarized acceptor hole should be $S_{\text{Tot}} = 5/2 - 1/2 = 2$, resulting from antiferromagnetic coupling between the Mn spin ($S_{\text{Mn}} = 5/2$) and the hole spin (s_h). If this “spin” is subject to an anisotropy landscape with energy barriers of 1 meV, it would take a magnetic field on the order of 10 T to revert its direction. Although for a Mn on surface the acceptor wavefunction is rather insensitive to the direction of the Mn magnetic moment, this does not seem to be the case for impurities located in the first 10 sub-layers below the surface. In particular, the acceptor partial DOS on (110) surface accessible from STM experiments is predicted to depend strongly on the direction of the magnetic moment. This would imply the possibility of controlling the STM tunneling current by rotating the Mn acceptor with a magnetic field. So far experiments carried out with magnetic fields up to 7 T do not find any dependence of the conductance for different directions of the magnetic field.⁵³ If the MAE barrier of the impurity is indeed 1 meV or larger, such fields might simply be not strong enough to rotate the direction of the spin.

V. ACKNOWLEDGMENTS

We would like to thank A. H. MacDonald, P. M. Koenraad, M. E. Flatté, O. Eriksson and J. Gupta for useful discussions. This work was supported by the Faculty of Natural Sciences at Linnaeus University, by the Swedish Research Council under Grant Numbers: 621-2007-5019 and 621-2010-3761 and by the Nordforsk research network: 08134, *Nanospintronics: theory and simulations*.

¹ H. Ohno, A. Shen, F. Matsukura, A. Oiwa, A. Endo, S. Katsumoto, and Y. Iye, Appl. Phys. Lett. **69**, 363 (1996).

² H. Ohno, Nat. Mater. **9**, 952 (2010).

³ T. Dietl, Nat. Mater. **9**, 956 (2010).

⁴ T. Dietl, H. Ohno, F. Matsukura, J. Cibert, and D. Ferrand, Science **287**, 1019 (2000).

⁵ A. H. MacDonald, P. Schiffer, and N. Samarth, Nat.

- Phys **4**, 195 (2005).
- ⁶ G. Zaránd and B. Jankó, Phys. Rev. Lett. **89**, 047201 (2002).
 - ⁷ C. Timm and A. H. MacDonald, Phys. Rev. B **71**, 155206 (2005).
 - ⁸ S. Hilbert and W. Nolting, Phys. Rev. B **71**, 113204 (2005).
 - ⁹ T. Jungwirth, K. Y. Wang, J. Mašek, K. W. Edmonds, J. König, J. Sinova, M. Polini, N. A. Goncharuk, A. H. MacDonald, M. Sawicki, et al., Phys. Rev. B **72**, 165204 (2005).
 - ¹⁰ T. Jungwirth, J. Sinova, J. Mašek, J. Kucera, and A. H. MacDonald, Rev. Mod. Phys. **78**, 809 (2006).
 - ¹¹ J. Zemen, J. Kučera, K. Olejník, and T. Jungwirth, Phys. Rev. B **80**, 155203 (2009).
 - ¹² J.-M. Tang and M. E. Flatté, Phys. Rev. Lett. **101**, 157203 (2008).
 - ¹³ K. S. Burch, D. D. Awschalom, and D. N. Basov, J. Magn. Magn. Mater. **320**, 3207 (2008).
 - ¹⁴ Y. Zhao, P. Mahadevan, and A. Zunger, Appl. Phys. Lett. **84**, 3753 (2004).
 - ¹⁵ P. Mahadevan, A. Zunger, and D. D. Sarma, Phys. Rev. Lett. **93**, 177201 (2004).
 - ¹⁶ A. Mikkelsen, B. Sanyal, J. Sadowski, L. Ouattara, J. Kanski, S. Mirbt, O. Eriksson, and E. Lundgren, Phys. Rev. B **70**, 085411 (2004).
 - ¹⁷ H. Ebert and S. Mankovsky, Phys. Rev. B **79**, 045209 (2009).
 - ¹⁸ K. Sato, L. Bergqvist, J. Kudrnovský, P. H. Dederichs, O. Eriksson, I. Turek, B. Sanyal, G. Bouzerar, H. Katayama-Yoshida, V. A. Dinh, et al., Rev. Mod. Phys. **82**, 1633 (2010).
 - ¹⁹ J. Mašek, F. Máca, J. Kudrnovský, O. Makarovskiy, L. Eaves, R. P. Campion, K. W. Edmonds, A. W. Rushforth, C. Foxton, B. L. Gallagher, et al., Phys. Rev. Lett. **105**, 227202 (2010).
 - ²⁰ S. Ohya, K. Takata, and M. Tanaka, Nat. Phys. **7**, 342 (2011).
 - ²¹ C. Śliwa and T. Dietl, Phys. Rev. B **83**, 245210 (2011).
 - ²² A. Richardella, P. Roushan, S. Mack, B. Zhou, D. A. Huse, D. D. Awschalom, and A. Yazdani, Science **327**, 665 (2010).
 - ²³ A. M. Yakunin, A. Y. Silov, P. M. Koenraad, J. H. Wolter, W. Van Roy, J. De Boeck, J.-M. Tang, and M. E. Flatté, Phys. Rev. Lett. **92**, 216806 (2004).
 - ²⁴ A. M. Yakunin, A. Y. Silov, P. M. Koenraad, J.-M. Tang, M. E. Flatté, W. Van Roy, J. De Boeck, and J. H. Wolter, Phys. Rev. Lett. **95**, 256402 (2005).
 - ²⁵ D. Kitchen, A. Richardella, J. M. Tang, M. E. Flatté, and A. Yazdani, Nature **442**, 436 (2006).
 - ²⁶ J. K. Garleff, C. Çelebi, W. Van Roy, J. M. Tang, M. E. Flatté, and P. M. Koenraad, Phys. Rev. B **78**, 075313 (2008).
 - ²⁷ A. Richardella, D. Kitchen, and A. Yazdani, Phys. Rev. B **80**, 045318 (2009).
 - ²⁸ C. Çelebi, J. K. Garleff, A. Y. Silov, A. M. Yakunin, P. M. Koenraad, W. Van Roy, J. M. Tang, and M. E. Flatté, Phys. Rev. Lett. **104**, 086404 (2010).
 - ²⁹ D. H. Lee and J. A. Gupta, Science **330**, 1807 (2010).
 - ³⁰ P. M. Koenraad and M. E. Flatté, Nat. Mat. **10**, 91 (2011).
 - ³¹ J.-M. Tang and M. E. Flatté, Phys. Rev. Lett. **92**, 047201 (2004).
 - ³² T. O. Strandberg, C. M. Canali, and A. H. MacDonald, Phys. Rev. B **80**, 024425 (2009).
 - ³³ J.-M. Tang and M. E. Flatté, Phys. Rev. B **72**, 161315 (2005).
 - ³⁴ J.-M. Tang and M. E. Flatté, Proc. SPIE **7398**, 73980 (2009).
 - ³⁵ T. O. Strandberg, C. M. Canali, and A. H. MacDonald, Phys. Rev. B **81**, 054401 (2010).
 - ³⁶ J. K. Garleff, A. P. Wijnheijmer, A. Y. Silov, J. van Bree, W. Van Roy, J.-M. Tang, M. E. Flatté, and P. M. Koenraad, Phys. Rev. B **82**, 035303 (2010).
 - ³⁷ A. Stroppa, X. Duan, M. Peressi, D. Furlanetto, and S. Modesti, Phys. Rev. B **75**, 195335 (2007).
 - ³⁸ J. P. Perdew, K. Burke, and M. Ernzerhof, Phys. Rev. Lett. **77**, 3865 (1996).
 - ³⁹ P. Blaha, K. Schwarz, G. K. H. Madsen, D. Kvasnicka, and J. Luitz, WIEN2k, An Augmented Plane Wave Plus Local Orbitals Program for Calculating Crystal properties (Vienna University of Technology, Austria) (2001).
 - ⁴⁰ J. M. Solar, E. Artacho, J. D. Gale, A. Garcia, J. Junquera, P. Ordejon, and D. Sanchez-Portal, J. Phys.: Condens. Matter **14**, 2745 (2002).
 - ⁴¹ D. D. Koelling and B. N. Harmon, J. Phys. C **10**, 3107 (1977).
 - ⁴² J. Schneider, U. Kaufmann, W. Wilkening, M. Baeumler, and F. Köhl, Phys. Rev. Lett. **59**, 240 (1987).
 - ⁴³ M. Linnarsson, E. Janzen, B. Monemar, M. Kleverman, and A. Thilderkvist, Phys. Rev. B **55**, 6938 (1997).
 - ⁴⁴ T. O. Strandberg, C. M. Canali, and A. H. MacDonald, Phys. Rev. Lett. **106**, 017202 (2011).
 - ⁴⁵ A. I. Liechtenstein, M. I. Katsnelson, V. P. Antropov, and V. A. Gubanov, J. Magn. Magn. Mater. **67**, 65 (1987).
 - ⁴⁶ P. Bruno, Phys. Rev. B **39**, 865 (1989).
 - ⁴⁷ D. J. Chadi, Phys. Rev. Lett. **41**, 1062 (1978).
 - ⁴⁸ P. Błoński, A. Lehnert, S. Dennler, S. Rusponi, M. Etzkorn, G. Moulas, P. Bencok, P. Gambardella, H. Brune, and J. Hafner, Phys. Rev. B **81**, 104426 (2010).
 - ⁴⁹ A. B. Shick, F. Máca, and A. I. Liechtenstein, Phys. Rev. B **79**, 172409 (2009).
 - ⁵⁰ These calculations, although in principle more accurate than the tight-binding calculations mentioned above, have the drawback that the surface area that can be simulated is rather small.
 - ⁵¹ In our calculations we employ one k -point only. The discrete spectrum is the solution of the Kohn-Sham equations for this k -point only.
 - ⁵² At the shortest Mn separation, the on-site Hubbard U might enhance a competitive superexchange mechanism that tends to favor antiferromagnetic coupling. Hence J decreases in this case.
 - ⁵³ P. M. Koenraad, private communication.